JCTC Journal of Chemical Theory and Computation

Article

pubs.acs.org/JCTC

# Evaluation of Approximate Exchange-Correlation Functionals in Predicting One-Bond $^{31}P-^{1}H$ NMR Indirect Spin−Spin Coupling Constants

Bimal Pudasaini and Benjamin G. Janesko*

Texas Christian University, 2800 South University Drive, Fort Worth, Texas 76129, United States

Supporting Information

**ABSTRACT:** This work benchmarks density functional theory, with several different exchange-correlation functionals, for prediction of isotropic one-bond phosphorus−hydrogen NMR spin−spin coupling constants (SSCCs). Our test set consists of experimental SSCCs from 30 diverse molecules representing multiple phosphorus bonding environments. The results suggest the importance of a balance between the choice of correlation functional and the admixture of nonlocal exchange. Overall, standard DFT methods appear to suffice for usefully accurate predictions of $^{31}P-^{1}H$ SSCCs.

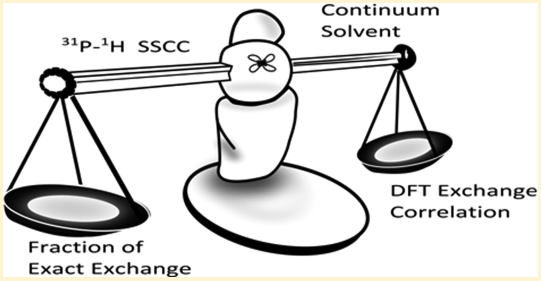


## 1. INTRODUCTION

Nuclear magnetic resonance (NMR) spectroscopy is one of the most widely used tools to identify molecular structures. NMR chemical shifts and spin−spin coupling constants (SSCCs) provide information on the chemical environment around nuclei. Chemical shifts are the resonance frequency of a given nuclear spin in an external magnetic field, evaluated relative to a reference molecule. SSCCs are reference- and external magnetic field-independent quantities arising from interactions of the magnetic dipole moments on different nuclei, modulated by electron−nuclear interactions.[1−4]

Calculated chemical shifts and SSCCs are often used to validate NMR spectral assignments.[5,6] Such calculations are particularly useful for ambiguous spectra and transient species.[6,7] There are many literature reports of calculated chemical shifts.[8−10] However, accurately predicting SSCCs is more challenging. High level ab initio calculations can reproduce experimental SSCCs.[2,4,11] However, their application to large molecules is limited by their computational cost. Density functional theory (DFT, vide infra) can provide a reasonable trade-off between cost and accuracy for modeling medium-sized to large molecules. This work benchmarks several DFT methods for predicting SSCCs of phosphorus−hydrogen bonds.

### 1.1. Evaluating Spin−Spin Coupling Constants.

We begin by briefly reviewing the definition and evaluation of nuclear spin−spin coupling constants. Details are in refs 1−4. The indirect spin−spin coupling tensor $\mathbf{J}_{N_1N_2}$ between nuclei $N_1$ and $N_2$ is

$$\mathbf{J}_{N_1N_2} = \frac{1}{h}\frac{\partial}{\partial \mathbf{I}_{N_1}}\frac{\partial}{\partial \mathbf{I}_{N_2}} E_0|_{\mathbf{I}_N=0} = \hbar\frac{\gamma_{N_1}\gamma_{N_2}}{2\pi}\mathbf{K}_{N_1N_2} \tag{1}$$

$E_0$ is the total ground state energy. $\gamma_N$ and $\mathbf{I}_N$ are the gyromagnetic ratio and spin angular momentum of nucleus $N$. $\mathbf{K}_{N_1N_2}$ is the reduced nuclear SSCC tensor. Only the isotropic value $^1/_3\ \mathrm{Tr}[\mathbf{K}_{N_1N_2}]$ contributes to the measured spectrum of orientationally averaged molecules.

Quantum chemical calculations of $\mathbf{K}_{N_1N_2}$ often use Ramsey's formalism[12] treating the effective interaction between two nuclear spins in the magnetic field of the electrons. The sum-over-states expression for the reduced coupling tensor is

$$\mathbf{K}_{N_1N_2} = \langle 0|h^{\mathrm{DSO}}_{N_1N_2}|0\rangle + 2\sum_{S\neq 0}\frac{\langle 0|h^{\mathrm{PSO}}_{N_1}|S\rangle\langle S|(h^{\mathrm{PSO}}_{N_2})^T|0\rangle}{E_0 - E_S} + 2\sum_{T}\frac{\langle 0|h^{FC}_{N_1} + h^{\mathrm{SD}}_{N_1}|T\rangle\langle T|(h^{FC}_{N_1})^T + (h^{\mathrm{SD}}_{N_1})^T|0\rangle}{E_0 - E_T} \tag{2}$$

Here $|0\rangle$, $|S\rangle$, and $|T\rangle$ are the ground electronic state, excited singlet states and excited triplet states. $E_n$ is the energy of the $n$th electronic state. $h^{\mathrm{DSO}}_{N_1N_2}$ is the diamagnetic spin−orbit (DSO) operator, a second-rank tensor reflecting the dependence of the molecular Hamiltonian on the nuclear magnetic moments:

$$h^{\mathrm{DSO}}_{N_1N_2} = \alpha^4\sum_j \frac{(\mathbf{r}^T_{jN_1}\mathbf{r}_{jN_2})\mathbf{I} - \mathbf{r}_{jN_1}r^T_{jN_2}}{r^3_{jN_1}r^3_{jN_2}} \tag{3}$$

$\alpha$ is the fine-structure constant and $\mathbf{r}^T_{jN}$ is the transpose of vector $\mathbf{r}_{jN}$ giving the separation between electron $j$ and nucleus $N$. $\mathbf{I}$ is the three-dimensional unit matrix. $h^{\mathrm{PSO}}_{N_1}$, $h^{\mathrm{FC}}_{N_1}$, $h^{\mathrm{SD}}_{N_1}$ are

Received: December 3, 2012
Published: February 15, 2013





dx.doi.org/10.1021/ct3010613 | J. Chem. Theory Comput. 2013, 9, 1443−1451

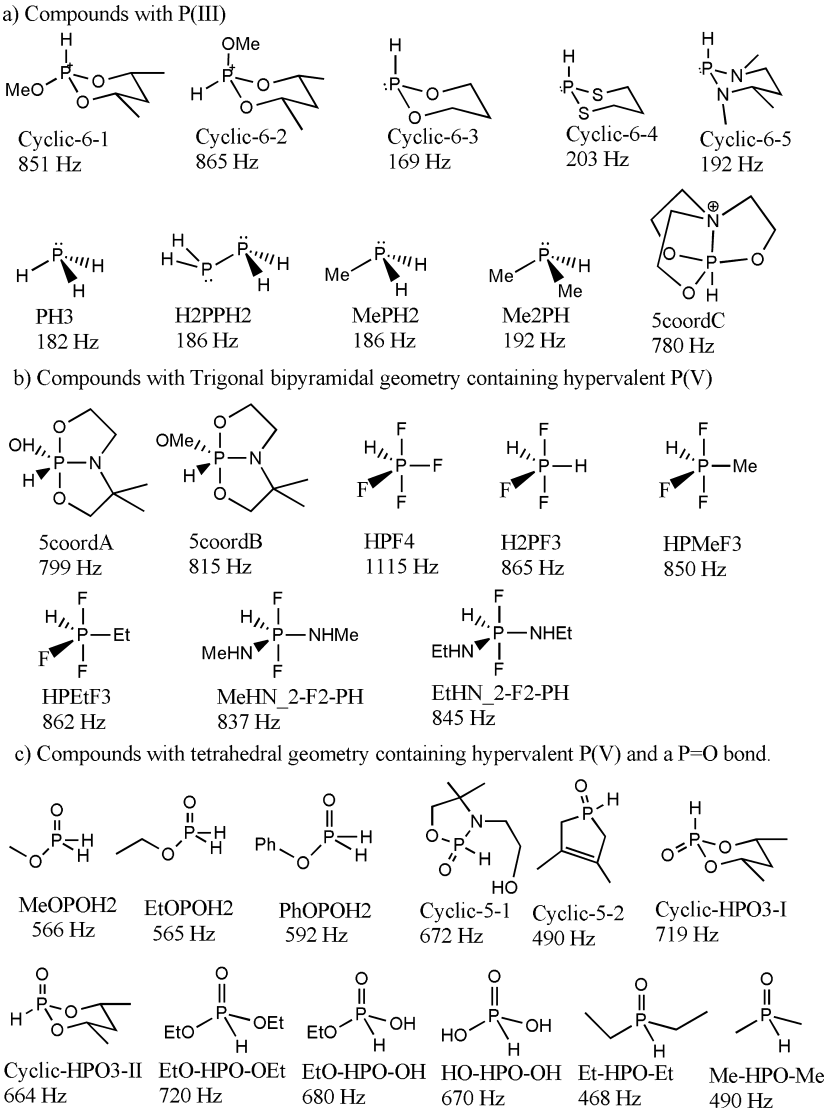


**Figure 1.** Compounds of the benchmark database. References to experimental SSCCs are in Table 1.

respectively the paramagnetic spin−orbit (PSO), Fermi-contact (FC), and spin-dipole (SD) operators, vectors defined as

$$h_{N_1}^{\mathrm{PSO}} = \alpha^2 \sum_j \frac{(\mathbf{r}_{jN_1} \times \mathbf{P}_j)}{r_{jN_1}^3} \tag{4}$$

$$h_1^{\mathrm{FC}} = \frac{8\pi\alpha^2}{3} \sum_j \delta(\mathbf{r}_{jN_1})\mathbf{S}_j \tag{5}$$

$$h_1^{\mathrm{SD}} = \alpha^2 \sum_j \frac{3(\mathbf{S}_j^T \mathbf{r}_{jN_1})\mathbf{r}_{jN_1} - \mathbf{r}_{jN_1}^2 \mathbf{S}_j}{r_{jN_1}^5} \tag{6}$$

$\mathbf{S}_j$ and $\mathbf{P}_j$ are respectively the operators for spin and linear momentum of electron $j$. $\delta(\mathbf{r}_{jN_1})$ is the Dirac delta function. DSO, PSO, FC, and SD terms may all make significant contributions to SSCCs.[13] In practice, we replace this sum-over-states formalism with analytic derivative calculations.[14−16]

**1.2. Density Functional Theory.** Kohn−Sham density functional theory treats the ground state of an $N$ electron system as a reference system of $N$ noninteracting fermions, corrected by a mean-field interaction and a formally exact[17] exchange-correlation (XC) density functional incorporating many-body effects.[18] Practical calculations typically require approximate XC functionals. The accuracy and computational cost of a DFT calculation largely depend on the choice of approximate functional and the basis set used for the reference system. A "Jacob's Ladder" of approximate XC functionals has been developed, with higher "rungs" incorporating more complicated ingredients and ideally giving higher accuracy.[19] The local spin-density approximation (LSDA) constructs the XC energy density at point $\mathbf{r}$ from the electron spin densities $\rho_\sigma(\mathbf{r})$, $\sigma = \uparrow,\downarrow$. Generalized gradient approximations (GGAs) incorporate $\nabla\rho_\sigma(\mathbf{r})$, giving a slightly higher cost[20] and improved treatments of many molecular properties.[21−23] Meta-GGAs incorporate the density Laplacian and/or the kinetic energy density of the noninteracting reference system. Meta-GGAs can have almost twice the cost of the LSDA[20] but often improve on GGAs.[21−23] The LSDA, GGAs, and meta-GGAs may be collectively referred to as "semilocal" functionals. Hybrid functionals incorporate a fraction of nonlocal exact exchange


dx.doi.org/10.1021/ct3010613 | J. Chem. Theory Comput. 2013, 9, 1443−1451

$$E_{X\sigma} = -\frac{1}{2}\int d^3\mathbf{r}\int d^3\mathbf{r}'\frac{|\gamma_\sigma(\mathbf{r},\mathbf{r}')|^2}{|\mathbf{r}-\mathbf{r}'|} \quad (7)$$

$\gamma_\sigma(\mathbf{r},\mathbf{r}') = \sum_i \phi_{i\sigma}(\mathbf{r})\phi^*_{i\sigma}(\mathbf{r}')$ is constructed from $\{\phi_{i\sigma}(\mathbf{r})\}$, the occupied spin−orbitals of the noninteracting reference system, which are typically expanded in a finite basis set. Global hybrids combine a fraction $0 < a < 1$ of exact exchange, a fraction $1 - a$ of a semilocal exchange functional and semilocal correlation.[24] Hybrids can accurately predict many properties including molecular geometries,[25] thermochemistry,[26−28] and reaction barriers.[29,30]

**1.3. DFT Calculations of SSCCs.** Several investigators have tested various basis sets and XC functionals for predicting SSCCs. Early studies on small data sets found that the B3LYP[31,32] global hybrid performed well.[14,15,33] Maximoff and co-workers found that several GGAs outperformed B3LYP for a larger set of C−H SSCCs.[20] Keal and co-workers showed that GGAs constructed to predict NMR chemical shieldings[34] gave variable performance for SSCCs.[35] Patchkovskii and co-workers showed that Kohn−Sham calculations incorporating the Krieger−Li−Iafrate approximation to the optimized effective potential (OEP)[36] and the Perdew−Zunger self-interaction correction[37] to the LSDA provided accurate chemical shieldings but variable performance for SSCCs.[38] Kaupp and co-workers have also explored NMR calculations with approximations to the OEP.[39] Keal and co-workers reproduced the results of Maximoff and co-workers, and showed that PBE is problematic for SSCCs involving N, O, and F atoms.[40] Witanowski and co-workers showed that B3PW91[32] accurately predicts the C−C SSCCs of substituted benzenes.[41] Suardíaz and co-workers found that B3LYP outperformed PBE for one-bond C−C SSCCs.[42]

Several studies have shown that DFT[14,15,38,43−47] and ab initio[11,48] calculations of SSCCs require large basis sets. In particular, the Fermi contact contribution requires large-exponent basis functions to model the electron density at the nucleus. This work follows Maximoff and co-workers[20] in using the contracted aug-cc-pVTZ-J basis set.[49,50] (Accurate treatments of phosphorus tautomerization energies would also require core polarization functions.[51])

**1.4. DFT Calculations of $^{31}$P−$^{1}$H SSCCs.** Phosphorus−hydrogen couplings are widely used in conformational analysis of biomolecules.[52] One-bond $^{31}$P−$^{1}$H SSCCs are particularly relevant to determining the structure of organophosphorus compounds. Such compounds' tautomerization and multiple redox states are critical to their chemistry.[53,54] NMR spectra can probe these aspects of phosphorus chemistry.[55,56] However, only a few computational studies have been used to support these assignments. Pecul and co-workers studied one-bond P−$X$ ($X$ = H, C, O, Se, and N) spin−spin couplings in dioxaphosphorinanes and found that DFT calculations gave reasonable predictions for the conformational dependence of SSCCs.[57] Wrackenmeyer found reasonable agreement between experiment and DFT calculations for P−C SSCCs.[58] Forgeron and co-workers compared relativistic and nonrelativistic DFT (GGA) calculations of P−P SSCCs and suggested that relativistic corrections were not essential.[59]

Here, we extend previous DFT benchmarks of SSCCs[14,15,20,33,35,41,42] to one-bond $^{31}$P−$^{1}$H couplings. We present a benchmark database of literature $^{31}$P−$^{1}$H SSCCs and tests of various approximate XC functionals. The results indicate that a functional's performance depends sensitively on the correlation functional and choice of exact exchange and that several standard functionals provide reasonable results.

## 2. COMPUTATIONAL DETAILS

Figure 1 lists the 30 molecules used in this study and their reported $^{31}$P−$^{1}$H SSCCs. Table 1 gives literature references for each. The molecules are categorized into three groups: compounds with P(III), with trigonal bipyramidal P(V), and with tetrahedral P(V) containing a P═O bond.

**Table 1. References for Experimental SSCCs of Molecules in Figure 1**

| cmpds | ref |
|---|---|
| MeOPOH2, EtOPOH2, PhOPOH2 | 53 |
| Cyclic-5-1, 5coordA, 5coordB | 82 |
| 5coordC | 83 |
| HPF4, H2PF3 | 84 |
| HPMeF3, HPEtF3 | 85 |
| MeHN2-F2-PH, EtHN2-F2-PH | 86 |
| Et-HPO-Et, Me-HPO-Me, Cyclic-5-2 | 87 |
| Cyclic-HPO3-I, Cyclic-HPO3-II | 88 |
| EtO-HPO-OEt, EtO-HPO-OH, HO-HPO-OH | 89 |
| Cyclic-6-1, Cyclic-6-2 | 90 |
| Cyclic-6-3, Cyclic-6-4, Cyclic-6-5 | 91 |
| PH3, H2PPH2 | 92 |
| MePH2, Me2PH | 93 |

Table 2 lists the 15 tested approximate XC functionals. PBE[60] is a nonempirical GGA. PBE0 is the corresponding (arguably nonempirical) global hybrid.[61−63] $\tau$-HCTH uses a gradient- and kinetic-energy-dependent expansion following Becke.[64−66] M06L, M06, and M06-2X use a similar but more complex functional form and respectively include 0%, 27%, and 54% exact exchange.[67,68] M06L and M06, but not M06-2X, also include meta-GGA exchange contributions similar to VSXC.[69] MPW1K includes a relatively large fraction of exact exchange $a$ = 0.428 and provides accurate chemical shifts.[70−72] The $\omega$B97X-D long-range-corrected hybrid[73] combines an empirical meta-GGA form[64] with different fractions of exact exchange at different $|\mathbf{r}-\mathbf{r}'|$,[74,75] as well as damped interatomic dispersion corrections.[76]

**Table 2. Tested Exchange-Correlation Density Functionals and References**

| XC | class | refs |
|---|---|---|
| PBE | GGA | 60 |
| BLYP | GGA | 94−96 |
| BP86 | GGA | 94 and 97 |
| mPWPW91 | GGA | 98−101 |
| M06L | meta-GGA | 67 |
| VSXC | meta-GGA | 69 |
| TPSS | meta-GGA | 102 |
| $\tau$-HCTH | meta-GGA | 66 |
| B3LYP | hybrid GGA | 94−96 |
| MPW1K | hybrid GGA | 70,71,98−101 |
| PBE0 | hybrid GGA | 62 and 63 |
| M06 | hybrid meta-GGA | 68 |
| M06-2X | hybrid meta-GGA | 68 |
| TPSSh | hybrid meta-GGA | 102 |
| $\omega$B97X-D | hybrid meta-GGA | 73 |


dx.doi.org/10.1021/ct3010613 | J. Chem. Theory Comput. 2013, 9, 1443−1451

$^{31}$P−$^{1}$H SSCCs are calculated as follows. Calculations use the Gaussian 09 electronic structure package.[77] Coupling constants are calculated using standard coupled-perturbed Kohn−Sham methods[13−15,43,44] and the aug-cc-pVTZ-J basis set.[49,50] Basis sets were obtained from the EMSL basis set exchange.[78,79] All calculations are nonrelativistic.[59] Calculations use the generalized Kohn−Sham formalism[80] with a nonlocal exchange potential in hybrid functionals. The semilocal XC energy density was numerically integrated using integration grids of 99 radial and 590 angular points per atom. Tests of M06 with much larger integration grids[81] gave comparable results (Supporting Information). Self-consistent field calculations used "tight" convergence criteria for total energies and densities (Gaussian keyword SCF = Tight).

Molecular geometries were optimized using B3LYP/6-31+G(3df,p) without any spatial symmetry restrictions. Conformational analyses were performed for each rotatable bond by manually scanning over dihedral angles using B3LYP/6-31+G(d,p) calculations and reoptimizing. Relative stabilities of boat, chair, and twist conformations in the cyclic compounds were also analyzed. Only the most stable conformer is selected for the NMR studies. Thermal effects on SSCCs are not explicitly included. However, compounds with multiple P−H bonds have their SSCCs averaged where appropriate. (For example, the two P−H SSCCs in **MeOPOH2** are averaged to account for rotational averaging of the P-OMe bond on the NMR time scale.) MAE, RMSD, and MSE respectively denote mean absolute error, root-mean-square deviation, and mean signed error. Signed errors are evaluated as calculated-reference.

Very accurate calculations of SSCCs require computationally expensive zero point and rovibrational corrections.[3,11] The benchmark study by Suardíaz and co-workers ignored these corrections.[42] Maximoff and co-workers added a 5 Hz correction to one-bond C−H SSCCs,[20] following the explicitly calculated corrections in ref 3. To our knowledge, such studies have not been performed on $^{31}$P−$^{1}$H SSCCs. We thus omit zero-point and rovibrational corrections. We also explore empirically determining such corrections from linear fits to experiment.

Rovibrational corrections are effectively corrections to the Born−Oppenheimer geometry. We can begin to estimate the error introduced by ignoring these corrections, by comparing how the $^{31}$P−$^{1}$H and C−H SSCCs vary with bond length. Figure 2 compares how the P−H SSCCs of $PH_3$ and **Me-HPO-Me** (Figure 1), and the C−H SSCCs of $CH_4$ and HCN, change with symmetric stretches of P−H and C−H bond lengths, respectively. The methane C−H SSCC decreases with bond elongation, consistent with ref 103. The absolute slope of SSCC vs bond length is comparable for both C−H bonds, consistent with the constant correction of Maximoff and co-workers.[20] The absolute slopes for P−H bonds are 1−2 times the value for C−H bonds. Thus, a very rough estimate is that rovibrational effects on $^{31}$P−$^{1}$H SSCCs are ∼1−2 times those of C−H bonds (i.e., around 5−10 Hz).

Accurate calculations of SSCCs also require consideration of solvent effects.[11,104] Our reference values are generally measured in solvent (Supporting Information). Several previous DFT benchmarks have directly compared gas-phase calculations to experiments in solvent.[20,33,42] We instead consider the role of continuum solvent effects, using a polarizable continuum model.[105,106] Calculations use continuum water solvent unless noted otherwise. Section 3.4 compares error statistics evaluated with continuum water solvent, chloroform solvent and no solvent model. All calculations use geometries optimized in continuum water.

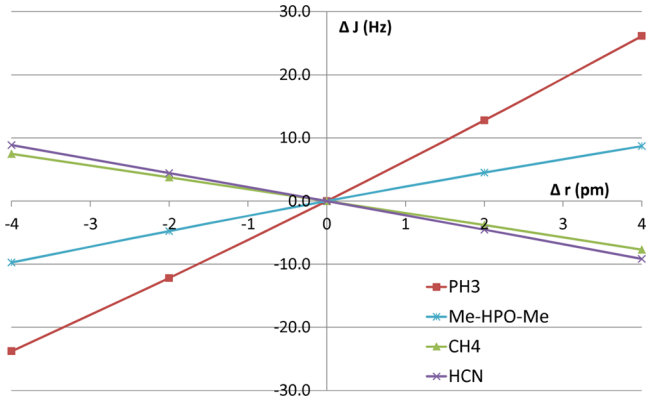


**Figure 2.** Spin−spin coupling constants as a function of molecular geometry. B3LYP/aug-cc-pVTZ-J $PH_3$ and Me-HPO-Me $^{31}$P−$^{1}$H SSCC vs P−H bond length, $CH_4$ and HCN $^{13}$C−$^{1}$H SSCC vs C−H bond length.

## 3. RESULTS AND DISCUSSION

**3.1. Results for Different Subsets.** Table 3 shows error statistics for the 10 P(III) compounds in Figure 1. For $PH_3$, the

**Table 3. Error Statistics (Hz) for SSCCs of the 10 P(III) Compounds in Figure 1**

| XC | MAE | RMSD | MSE | max(+) | max(-) |
|---|---|---|---|---|---|
| PBE | 45.5 | 48.2 | −44.2 | 6.2 | −63.3 |
| BLYP | 36.3 | 41.6 | −4.9 | 87.2 | −44.2 |
| BP86 | 43.2 | 45.6 | −41.0 | 11.1 | −59.6 |
| mPWPW91 | 40.9 | 42.9 | −36.6 | 21.9 | −57.1 |
| M06L | 21.6 | 28.6 | 19.9 | 57.2 | −7.4 |
| VSXC | 28.1 | 33.6 | −26.0 | 10.5 | −71.0 |
| TPSS | 20.7 | 31.5 | 19.5 | 78.0 | −3.3 |
| $\tau$-HCTH | 21.2 | 24.2 | 12.0 | 38.1 | −33.5 |
| B3LYP | 21.4 | 30.7 | 4.9 | 74.9 | −22.8 |
| MPW1K | 8.6 | 12.9 | 0.7 | 32.4 | −15.7 |
| PBE0 | 24.0 | 25.4 | −20.6 | 17.2 | −40.0 |
| M06 | 65.6 | 71.1 | 65.6 | 128.4 | 37.7 |
| M06−2X | 31.2 | 33.1 | 31.2 | 50.3 | 14.4 |
| TPSSh | 26.8 | 36.1 | 36.8 | 83.3 | 6.1 |
| $\omega$B97X-D | 17.7 | 23.8 | −17.7 | −2.9 | −58.6 |

B3LYP/aug-cc-pVTZ-J $^{31}$P−$^{1}$H SSCC are 171.6 Hz in vacuum and 181.5 Hz in aqueous solvent. These are comparable to previously reported 163.96 Hz from gas-phase B3LYP/UGBS2P calculations,[44] 170 Hz from gas-phase B3LYP in a large basis set,[33] and 168.4 Hz from gas-phase B3LYP/aug-cc-pvTZ-J.[49] (Slight differences arise in part from different geometries.)

Overall, the PBE GGA performs rather poorly, consistent with its poor treatment of SSCCs involving electronegative first-row atoms.[40] The tested meta-GGAs generally outperform the GGAs. The best semilocal functionals are the empirical M06L and $\tau$-HCTH meta-GGAs. The PBE0 and MPW1K global hybrids are significantly more accurate than the "parent" functionals PBE and mPWPW91. However, TPSSh is somewhat worse than TPSS. The Minnesota functionals have a nonsystematic behavior with admixture of exact exchange: M06 gives the largest maximum error, and an overall MAE


dx.doi.org/10.1021/ct3010613 | J. Chem. Theory Comput. 2013, 9, 1443−1451

significantly above M06L or M06-2X. We speculate that this may arise from the VSXC terms in M06, or the different empirical parameters.[68] MPW1K and ωB97X-D are overall most accurate for P(III) compounds.

Table 4 shows error statistics for the eight hypervalent pentacoordinated P(V) compounds with trigonal bipyramidal geometries in Figure 1. The results are less systematic than for P(III) compounds. The PBE and BLYP GGAs are again rather inaccurate. The tested meta-GGAs again generally outperform GGAs, though their overall performance is worse than for P(III) compounds. Admixture of exact exchange is not as beneficial. While the PBE0 global hybrid is rather accurate, B3LYP is inaccurate and the MPW1K and TPSSh hybrids are worse than their parent functionals. M06 is again significantly less accurate than M06-L or M06−2X. MPW1K and ωB97X-D again provide reasonable performance, though the overall lowest errors are achieved with PBE0 and τ-HCTH.

**Table 4. Error Statistics (Hz) for SSCCs of the Eight Trigonal Bipyramidal P(V) Compounds in Figure 1**

| XC | MAE | RMSD | MSE | max(+) | max(−) |
|---|---|---|---|---|---|
| PBE | 40.4 | 43.7 | −40.4 | −12.3 | −59.3 |
| BLYP | 48.1 | 51.6 | 48.1 | 74.1 | 24.3 |
| BP86 | 35.5 | 39.2 | −35.5 | −7.6 | −55.7 |
| mPWPW91 | 24.1 | 28.2 | −22.9 | 4.6 | −42.6 |
| M06L | 30.9 | 35.4 | −3.5 | 42.0 | −58.3 |
| VSXC | 37.0 | 42.1 | −37.0 | −8.1 | −71.0 |
| TPSS | 40.5 | 43.8 | 40.5 | 63.9 | 17.8 |
| τ-HCTH | 14.9 | 16.1 | −5.8 | 16.6 | −23.6 |
| B3LYP | 54.0 | 56.4 | 54.0 | 73.6 | 30.5 |
| MPW1K | 27.8 | 31.3 | 27.8 | 48.3 | 4.8 |
| PBE0 | 14.5 | 15.4 | −6.4 | 13.6 | −24.7 |
| M06 | 79.1 | 88.4 | 79.1 | 143.3 | 22.0 |
| M06-2X | 41.5 | 45.2 | 41.5 | 62.8 | 11.1 |
| TPSSh | 55.1 | 57.6 | 55.1 | 75.2 | 30.0 |
| ωB97X-D | 30.7 | 33.7 | −30.7 | −11.3 | −46.6 |

Table 5 shows error statistics for the 12 tetracoordinated P(V) compounds with P═O bonds in Figure 1. The results are again consistent with previous work. B3LYP/aug-cc-pVTZ-J SSCCs for Cyclic-HPO3-I and Cyclic-HPO3-I are respectively 769.8 and 698.8 Hz in solvent, consistent with gas-phase B3LYP/aug-cc-pVTZ-J values 758 and 672 Hz reported previously.[57] The trends are similar to Tables 3 and 4. The PBE and BP86 GGAs and M06 hybrid meta-GGA perform poorly. Admixture of exact exchange makes PBE0 significantly more accurate than PBE. The most reliable functionals are MPW1K, M06-L, and τ-HCTH.

**Table 5. Error Statistics (Hz) for SSCCs of the 12 Tetrahedral P(V) = O Compounds in Figure 1**

| XC | MAE | RMSD | MSE | max(+) | max(−) |
|---|---|---|---|---|---|
| PBE | 47.0 | 51.4 | −44.3 | 16.6 | −76.5 |
| BLYP | 33.5 | 41.2 | 17.9 | 93.4 | −33.3 |
| BP86 | 44.0 | 48.5 | −40.4 | 21.3 | −74.3 |
| mPWPW91 | 37.3 | 42.5 | −32.1 | 31.2 | −67.4 |
| M06L | 20.9 | 24.9 | 0.0 | 59.0 | −30.6 |
| VSXC | 35.6 | 38.4 | −31.8 | 22.9 | −57.6 |
| TPSS | 26.9 | 34.2 | 12.2 | 81.2 | −31.6 |
| τ-HCTH | 18.6 | 23.3 | −6.3 | 49.0 | −34.0 |
| B3LYP | 33.5 | 40.9 | 23.5 | 94.4 | −23.4 |
| MPW1K | 19.4 | 25.5 | 5.2 | 64.5 | −28.5 |
| PBE0 | 26.8 | 31.4 | −19.1 | 40.1 | −51.3 |
| M06 | 58.7 | 65.5 | 58.7 | 123.9 | 14.3 |
| M06−2X | 26.9 | 34.4 | 22.0 | 83.6 | −15.6 |
| TPSSh | 31.9 | 39.2 | 22.6 | 91.7 | −21.9 |
| ωB97X-D | 32.5 | 36.2 | −27.9 | 27.9 | −58.4 |

**3.2. Overall Results.** Table 6 summarizes the error statistics for all 30 molecules in Figure 1. The table shows statistical errors from uncorrected values, as well as the results of a linear fit to the experimental data. Figure 3 illustrates the calculated and experimental SSCCs and the corresponding linear fits for MPW1K and τ-HCTH. The overall trends are similar to those discussed above. Functionals from all rungs of Jacob's Ladder can provide reasonable results. τ-HCTH, MPW1K, PBE0, M06-L, and ωB97X-D all give reasonable accuracy.

The linear fits in Table 6 improve several of the worst-performing functionals. Most functionals give similar $R^2$ values, though MPW1K is again the most accurate. Most functionals also give fitted slopes near 1. However, the fitted intercepts vary significantly, with the tested GGAs all requiring constant shifts >50 Hz. These shifts are in some ways similar to the 5 Hz shift used by Maximoff and co-workers to account for zero-point and rovibrational corrections[20] but also account for limitations of the tested functional.

**3.3. Role of the DFT XC Functional.** The results in Tables 3−6 show that functionals from all rungs of Jacob's Ladder can provide reasonable $^{31}P-^{1}H$ SSCCs. This suggests that a given functional's performance depends in a complicated way on its semilocal ingredients and fraction of exact exchange. We attempt to rationalize this by evaluating the $^{31}P-^{1}H$ spin−spin coupling in $PH_3$ as a function of systematic changes in the admixture of exact exchange and the choice of semilocal exchange and correlation. All calculations use continuum solvent and B3LYP/6-31+G(3df,p) geometries to isolate the effect of the XC functional. Figure 4 shows the calculated $^{31}P-^{1}H$ SSCC plotted as a function of the fraction $a$ of exact exchange. Results are shown for global hybrids combining B88,[94] PBE,[60] mPW,[98] or TPSS[102] exchange with PBE[60] or LYP[95,96] correlation. Global hybrids with LYP correlation all converge to the HF-LYP value at $a = 1$, and global hybrids with PBE correlation converge to the HF-PBE value at $a = 1$.

The SSCCs in Figure 4 strongly depend on the admixture of exact exchange, with increasing fractions of exact exchange increasing the coupling. Hartree−Fock theory is known to underestimate triplet excitation energies, leading to large FC and SD contributions (eq 2) and overestimated SSCCs.[4,47] (Even high-level ab initio SSCCs can have large errors in the vicinity of triplet instabilities.[107]) Figure 5 illustrates the individual PSO, DSO, SD, and FC contributions to $PH_3$ SSCCs predicted by BLYP global hybrids. The FC and SD terms increase in magnitude with exact exchange admixture $a$, consistent with an increasing underestimate of triplet excitations. Helgaker and co-workers reported a similar dependence on $a$ for other small molecules.[15] Molecules with large PSO contributions, including $N_2$ and CO,[38] showed a more complicated dependence on $a$.[15] However, test calculations on 10 small molecules from our test set show that Hartree−Fock theory and HF-LYP always tend to overestimate SSCCs (Supporting Information). This is consistent with Kupka and co-workers, who showed that the M06-HF functional containing 100% exact exchange overestimates SSCCs of several small molecules.[45]


dx.doi.org/10.1021/ct3010613 | J. Chem. Theory Comput. 2013, 9, 1443−1451

**Table 6. Combined Error Statistics (Hz) for SSCCs of all 30 Molecules in Figure 1, along with Slope (Unitless), Intercept (Hz), and $R^2$ (Unitless) from a Linear Fit to Experimental Data**

| XC | MAE | RMSD | MSE | max(+) | max(−) | slope | intercept | $R^2$ |
|---|---|---|---|---|---|---|---|---|
| PBE | 44.8 | 47.9 | −43.2 | 16.6 | −76.5 | 0.972 | 59.1 | 0.9941 |
| BLYP | 38.3 | 45.1 | 18.4 | 93.4 | −44.2 | 0.885 | 53.2 | 0.9938 |
| BP86 | 41.5 | 44.6 | −39.3 | 21.3 | −74.3 | 0.969 | 57.0 | 0.9940 |
| mPWPW91 | 35.0 | 38.5 | −31.1 | 31.2 | −67.4 | 0.954 | 57.6 | 0.9942 |
| M06L | 23.8 | 29.9 | 5.7 | 59.0 | −58.3 | 0.980 | 6.6 | 0.9888 |
| VSXC | 33.5 | 38.2 | −31.2 | 22.9 | −71.0 | 1.013 | 23.9 | 0.9936 |
| TPSS | 28.4 | 36.9 | 22.2 | 81.2 | −31.6 | 0.937 | 17.4 | 0.9929 |
| $\tau$-HCTH | 18.5 | 21.5 | −0.1 | 49.0 | −34.0 | 1.023 | −13.6 | 0.9937 |
| B3LYP | 35.3 | 44.0 | 25.4 | 94.4 | −23.4 | 0.903 | 35.8 | 0.9948 |
| MPW1K | 18.0 | 24.4 | 9.7 | 64.5 | −28.5 | 0.954 | 18.3 | 0.9955 |
| PBE0 | 22.6 | 24.9 | −16.2 | 40.1 | −51.3 | 0.967 | 35.6 | 0.9954 |
| M06 | 66.4 | 75.7 | 66.4 | 143.3 | 14.3 | 0.933 | −21.3 | 0.9899 |
| M06-2X | 32.2 | 37.9 | 30.3 | 83.6 | −15.6 | 0.970 | −11.0 | 0.9944 |
| TPSSh | 36.4 | 45.3 | 32.7 | 91.7 | −21.9 | 0.929 | 12.3 | 0.9935 |
| $\omega$B97X-D | 27.1 | 31.7 | −25.2 | 27.9 | −58.6 | 1.017 | 15.4 | 0.9949 |

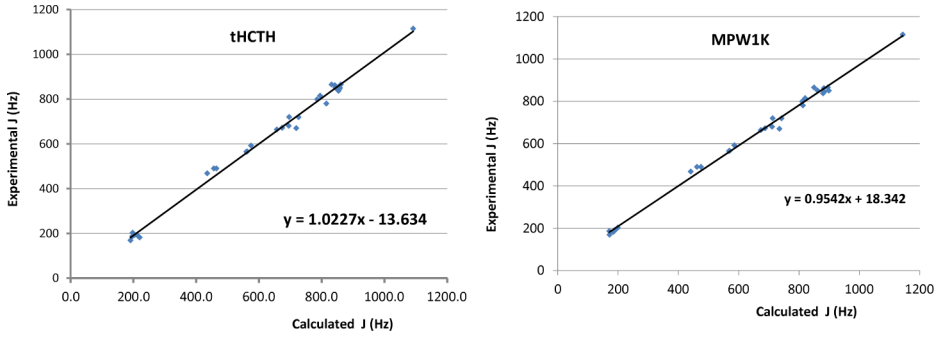


**Figure 3.** Calculated vs experimental SSCCs (Hz) for all molecules in Figure 1 and linear fit.

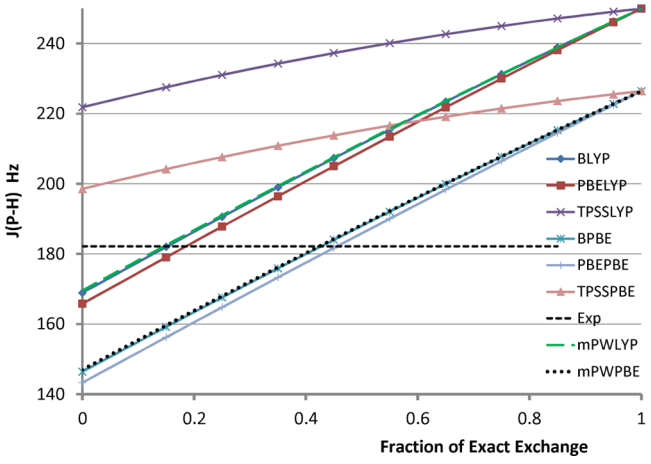


**Figure 4.** Calculated $^{31}P-^{1}H$ SSCCs in $PH_3$ for several global hybrids, plotted as a function of the fraction of exact exchange. The experimental coupling is shown as a horizontal line.

The SSCCs in Figure 4 depend less strongly on the choice of semilocal exchange. The B88, PBE, and mPW GGAs give nearly overlapping curves, with all three GGAs tending to underestimate SSCCs in the absence of exact exchange. However, the TPSS meta-GGA for exchange gives rather large couplings. This is consistent with the observation that TPSS gives a large positive mean signed error in Tables 3−6 and that the TPSSh global hybrid gives an even more positive MSE. Finally, the spin−spin coupling depends fairly strongly on the choice of semilocal correlation functional. LYP correlation gives SSCCs ∼ 20 Hz larger than PBE correlation.

Combining these effects, Figure 4 shows that GGA hybrids using LYP correlation best reproduce experiment for $PH_3$ with $a \sim 0.15$, while GGA hybrids using PBE correlation best reproduce experiment with $a \sim 0.40$. This is reasonably consistent with Tables 3−6. Accurate methods include PBE0 (PBE exchange and correlation, $a = 0.25$) and MPW1K (mPW exchange, PW91 correlation (similar to PBE correlation), $a = 0.428$).

**3.4. Role of Continuum Solvent.** Table 7 compares error statistics from gas-phase vs continuum solvent calculations. Results are presented for SSCCs of 10 small molecules from the test set: **HPEtF3**, **PH3**, **H2PPH2**, **MePH2**, **Me2PH**, **MeOPH2**, **EtOPH2**, **Me-HPO-Me**, **Et-HPO-Et**, **HPF4**. Calculations use the same geometries as above to isolate the effect of solvent on response properties. Results are presented for SSCCs calculated in the gas phase and with continuum chloroform or water solvent. Solvent corrections tend to increase individual SSCCs by ∼10−100 Hz (Supporting Information). The solvent corrections improve most of the tested functionals' agreement with experiment, and generally do not change their relative ordering. This is consistent with previous studies showing that continuum solvent tends to improve SSCCs.[108,108,109] Functionals such as TPSSh that strongly overestimate SSCCs tend to be improved by omitting solvent corrections, presumably due to fortuitous error cancellation. Using BLYP, M06L, TPSS, M062x, M06, and


dx.doi.org/10.1021/ct3010613 | J. Chem. Theory Comput. 2013, 9, 1443−1451

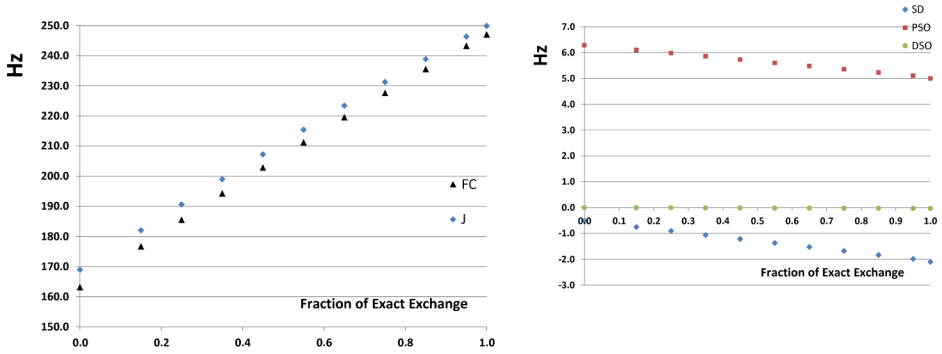


**Figure 5.** (Left) Calculated total and FC contribtion to $^{31}P-^{1}H$ SSCCs in $PH_3$, for global hybrids of BLYP, plotted as a function of the fraction of exact exchange. (Right) Same for SD, PSO, and DSO contributions.

**Table 7. MAE (Hz) for 10 Representative SSCCs, Gas-Phase and Continuum Solvent Calculations**

| XC | gas | $CHCl_3$ | water |
|---|---|---|---|
| PBE | 75.4 | 61.6 | 55.0 |
| BLYP | 28.1 | 25.2 | 27.3 |
| BP86 | 71.9 | 58.0 | 51.4 |
| mPWPW91 | 66.0 | 51.9 | 45.2 |
| M06L | 27.3 | 12.3 | 15.2 |
| VSXC | 59.3 | 46.4 | 40.2 |
| TPSS | 21.3 | 16.4 | 20.6 |
| $\tau$-HCTH | 34.5 | 25.7 | 21.8 |
| B3LYP | 20.1 | 20.8 | 22.7 |
| MPW1K | 25.6 | 17.0 | 12.9 |
| PBE0 | 49.5 | 34.3 | 27.1 |
| M06 | 34.3 | 50.7 | 60.3 |
| M06-2X | 20.1 | 25.1 | 30.1 |
| TPSSh | 16.5 | 21.5 | 26.5 |
| $\omega$B97X-D | 51.1 | 36.4 | 29.4 |

TPSSh, implicit continuum solvent of chloroform is preferred over water for the 10 test molecules.

## 4. CONCLUSION

We benchmark 15 different approximate XC functionals against a database of of 30 experimental one-bond $^{31}P-^{1}H$ NMR spin–spin coupling constants. Systematic analysis indicates that accuracy for SSCCs depends sensitively on the choice of semilocal correlation functional and the admixture of exact exchange, and to a lesser extent on the semilocal exchange functional and continuum solvent model. Accurate results are obtained at multiple levels on "Jacob's Ladder",[19] with the MPW1K global hybrid and the $\tau$-HCTH meta-GGA providing some of the best results. The PBE GGA is rather inaccurate, contrasting with its accurate treatment of C–H SSCCs[20] and consistent with its poor performance for SSCCs involving electronegative first-row atoms.[35] We conclude that standard DFT methods can provide useful accuracy for predicting $^{31}P-^{1}H$ SSCCs.

## ■ ASSOCIATED CONTENT

### Supporting Information

Calculated SSCCs, geometries and sources for experimental values. This material is available free of charge via the Internet at http://pubs.acs.org/.

## ■ AUTHOR INFORMATION

### Corresponding Author

*E-mail: b.janesko@tcu.edu.

### Notes

The authors declare no competing financial interest.

## ■ ACKNOWLEDGMENTS

This work was supported by funds from Texas Christian University. The authors thank Jean-Luc Montchamp for useful comments.

## ■ REFERENCES

(1) Fukui, H. *Prog. Nucl. Magn. Reson. Spectrosc.* **1999**, *35*, 267–294.
(2) Helgaker, T.; Jaszunski, M.; Ruud, K. *Chem. Rev.* **1999**, *99*, 293–352.
(3) Ruden, T. A.; Lutnïs, O. B.; Helgaker, T.; Ruud, K. *J. Chem. Phys.* **2003**, *118*, 9572.
(4) Helgaker, T.; Lodewyk, M. W.; Pecul, M. *Prog. Nucl. Magn. Reson. Spectrosc.* **2008**, *53*, 249–268.
(5) Lodewyk, M. W.; Soldi, C.; Jones, P. B.; Olmstead, M. M.; Rita, J.; Shaw, J. T.; Tantillo, D. J. *J. Am. Chem. Soc.* **2012**, *134*, 18550–18553.
(6) Bifulco, G.; Dambruoso, P.; Gomez-Paloma, L.; Riccio, R. *Chem. Rev.* **2007**, *107*, 3744–3779.
(7) Saielli, G.; Bagno, A. *Org. Lett.* **2009**, *11*, 1409–1412.
(8) Lodewyk, M. W.; Siebert, M. R.; Tantillo, D. J. *Chem. Rev.* **2012**, *112*, 1839–1862.
(9) Wullen, C. V. *Phys. Chem. Chem. Phys.* **2000**, *2*, 2137–2144.
(10) Chernyshev, K. A.; Krivdin, L. B. *Rus. J. Org. Chem.* **2010**, *46*, 785–790.
(11) Oddershede, J.; Geerten, J.; Scuseria, G. E. *J. Phys. Chem.* **1988**, *92*, 3056–3059.
(12) Ramsey, N. F. *Phys. Rev.* **1953**, *91*, 303–307.
(13) Barone, V.; Peralta, J. E.; Contreras, R.; Snyder, J. P. *J. Phys. Chem. A* **2002**, *106*, 5607–5612.
(14) Sychrovský, V.; Gräfstein, J.; Cremer, D. *J. Chem. Phys.* **2000**, *113*, 3530–3547.
(15) Helgaker, T.; Watson, M.; Handy, N. C. *J. Chem. Phys.* **2000**, *113*, 9402–9409.
(16) Autschbach, J.; Ziegler, T. *J. Chem. Phys.* **2000**, *113*, 936–947.
(17) Hohenberg, P.; Kohn, W. *Phys. Rev.* **1964**, *B136*, 864.
(18) Kohn, W.; Sham, L. *Phys. Rev.* **1965**, *140*, A1133.
(19) Perdew, J. P.; Schmidt, K. In *Density Functional Theory and its Application to Materials*; Van Doren, V., Van Alsenoy, C., Geerlings, P., Eds.; American Institute of Physics: Melville, NY , 2001; pp 1–20.
(20) Maximoff, S. N.; Peralta, J. E.; Barone, V.; Scuseria, G. E. *J. Chem. Theory Comput.* **2005**, *1*, 541–545.
(21) Cohen, A. J.; Mori-Sanchez, P.; Yang, W. *Chem. Rev.* **2012**, *112*, 289–320.

(22) Sameera, W. M. C.; Pantazis, D. A. *J. Chem. Theory Comput.* **2012**, *8*, 2630−2645.
(23) Riley, K. E.; Pitonak, M.; Jurecka, P.; Hobza, P. *Chem. Rev.* **2010**, *110*, 5023−5063.
(24) Becke, A. D. *J. Chem. Phys.* **1993**, *98*, 1372.
(25) Staroverov, V. N.; Scuseria, G. E.; Tao, J.; Perdew, J. P. *J. Chem. Phys.* **2003**, *119*, 12129.
(26) Karton, A.; Martin, J. M. L. *Mol. Phys.* **2012**, *110*, 2477−2491.
(27) Goerigk, L.; Grimme, S. *J. Chem. Theory Comput.* **2010**, *6*, 107−126.
(28) Riley, K. E.; Op't Holt, B. T.; Merz, K. E., Jr. *J. Chem. Theory Comput.* **2007**, *3*, 407.
(29) Tishchenko, O.; Truhlar, D. G. *J. Phys. Chem. Lett.* **2012**, *3*, 2834−2839.
(30) Andersson, S.; Grüning, M. *J. Phys. Chem. A* **2004**, *108*, 7621.
(31) Stephens, P. J.; Devlin, F. J.; Chabalowski, C. F.; Frisch, M. J. *J. Phys. Chem.* **1994**, *98*, 11623−11627.
(32) Becke, A. D. *J. Chem. Phys.* **1993**, *98*, 5648−5652.
(33) Lantto, P.; Vaara, J.; Helgaker, T. *J. Chem. Phys.* **2002**, *117*, 5998−6009.
(34) Keal, T. W.; Tozer, D. J. *J. Chem. Phys.* **2003**, *119*, 3015−3024.
(35) Keal, T. W.; Tozer, D. J.; Helgaker, T. *Chem. Phys. Lett.* **2004**, *391*, 374−379.
(36) Krieger, J. B.; Li, Y.; Iafrate, G. J. *Phys. Rev. A* **1992**, *46*, 5453.
(37) Perdew, J. P.; Zunger, A. *Phys. Rev. B* **1981**, *23*, 5048−5078.
(38) Patchkovskii, S.; Autschbach, J.; Ziegler, T. *J. Chem. Phys.* **2001**, *115*, 26−42.
(39) Arbuznikov, A. V.; Kaupp, M. *Chem. Phys. Lett.* **2004**, *386*, 8.
(40) Keal, T. W.; Helgaker, T.; Sałek, P.; Tozer, D. J. *Chem. Phys. Lett.* **2006**, *425*, 163−166.
(41) Witanowski, M.; Kamieńska-Trela, K.; Biedrzycka, Z. *J. Mol. Struct.* **2007**, *844*−*845*, 13−20.
(42) Suardaz, R.; Prez, C.; Crespo-Otero, R.; de la Vega, J. M. G.; Fabián, J. S. *J. Chem. Theory Comput.* **2008**, *4*, 448−456.
(43) Peralta, J. E.; Scuseria, G. E.; Cheeseman, J. R.; Frisch, M. J. *Chem. Phys. Lett.* **2003**, *375*, 452−458.
(44) Deng, W.; Cheeseman, J. R.; Frisch, M. J. *J. Chem. Theory Comput.* **2006**, *2*, 1028−1037.
(45) Kupka, T. *Chem. Phys. Lett.* **2008**, *461*, 33−37.
(46) Kupka, T.; Stachów, M.; Nieradka, M.; Kaminsky, J.; Pluta, T. *J. Chem. Theory Comput.* **2010**, *6*, 1580−1589.
(47) Kupka, T.; Nieradka, M.; Stachow, M.; Pluta, T.; Nowak, P.; Kjaer, H.; Kongsted, J.; Kaminsky, J. *J. Phys. Chem. A* **2012**, *116*, 3728−3738.
(48) Helgaker, T.; Jasuński, M.; Ruud, K.; Górska, A. *Theor. Chem. Acc.* **1998**, *99*, 175−182.
(49) Provasi, P. F.; Sauer, S. P. A. *J. Chem. Phys.* **2010**, *133*, 054308.
(50) Provasi, P. F.; Aucar, G. A.; Sauer, S. P. A. *J. Chem. Phys. Lett.* **2003**, *119*, 1324.
(51) Wesolowski, S. S.; Brinkmann, N. R.; Valeev, E. F.; Schaefer, H. F., III; Repasky, M. P.; Jorgensen, W. L. *J. Chem. Phys.* **2002**, *116*, 112−122.
(52) Wu, Z.; Delagilio, F.; Tjandra, N.; Zhurkin, V. B.; Bax, A. *J. Biomol. NMR* **2003**, *26*, 297−315.
(53) Deprele, S.; Montchamp, J.-L. *J. Organomet. Chem.* **2002**, *643*−*644*, 154−163.
(54) Coudray, L.; Montchamp, J.-L. *Eur. J. Org. Chem.* **2008**, 3601−3613.
(55) Yakhvarov, D.; Caporali, M.; Gonsalvi, L.; Latypov, S.; Mirabello, V.; Rizvanov, I.; Sinyashin, O.; Stoppioni, P.; Peruzzini, M. *Angew. Chem., Int. Ed.* **2011**, *50*, 5370−5373.
(56) Hersh, W. H.; Lam, S. T.; Moskovic, D. J.; Panagiotakis, A. J. *J. Org. Chem.* **2012**, *77*, 4968−4979.
(57) Pecul, M.; Urbańczyk, M.; Wodyński, A.; Jasuński, M. *Magn. Reson. Chem.* **2011**, *49*, 399−404.
(58) Wrackmeyer, B. *Z. Naturforsch., B* **2003**, *58*, 1041−1044.
(59) Forgeron, M. A. M.; Gee, M.; Wasylishen, R. *J. Phys. Chem. A* **2004**, *108*, 4895−4908.
(60) Perdew, J. P.; Burke, K.; Ernzerhof, M. *Phys. Rev. Lett.* **1996**, *77*, 3865−3868.
(61) Perdew, J. P.; Ernzerhof, M.; Burke, K. *J. Chem. Phys.* **1996**, *105*, 9982−9985.
(62) Adamo, C.; Barone, V. *J. Chem. Phys.* **1999**, *110*, 6158−6170.
(63) Ernzerhof, M.; Scuseria, G. E. *J. Chem. Phys.* **1999**, *110*, 5029−5036.
(64) Becke, A. D. *J. Chem. Phys.* **1997**, *107*, 8554.
(65) Becke, A. D. *J. Chem. Phys.* **1998**, *109*, 2092−2098.
(66) Boese, A. D.; Handy, N. C. *J. Chem. Phys.* **2002**, *116*, 9559−9569.
(67) Zhao, Y.; Truhlar, D. G. *J. Chem. Phys.* **2006**, *125*, 194101.
(68) Zhao, Y.; Truhlar, D. G. *Theor. Chem. Acc.* **2008**, *120*, 215−241.
(69) Voorhis, T. V.; Scuseria, G. E. *J. Chem. Phys.* **1998**, *109*, 400−410.
(70) Lynch, B. J.; Fast, P. l.; Harris, M.; Truhlar, D. G. *J. Phys. Chem. A* **2000**, *104*, 4811.
(71) Lynch, B. J.; Zhao, Y.; Truhlar, D. G. *J. Phys. Chem. A* **2003**, *107*, 1384.
(72) Maryasin, B.; Zipse, H. *Phys. Chem. Chem. Phys.* **2011**, *13*, 5150−5158.
(73) Chai, J.-D.; Head-Gordon, M. *Phys. Chem. Chem. Phys.* **2008**, *10*, 6615−6620.
(74) Savin, A. In *Recent Developments and Applications of Modern Density Functional Theory*; Seminario, J. M., Ed.; Elseveir: Amsterdam, 1996; p 327.
(75) Leininger, T.; Stoll, H.; Werner, H.-J.; Savin, A. *Chem. Phys. Lett.* **1997**, *275*, 151.
(76) Grimme, S. *J. Comput. Chem.* **2004**, *25*, 1463.
(77) Frisch, M. J.; Trucks, G. W.; Schlegel, H. B.; Scuseria, G. E.; Robb, M. A.; Cheeseman, J. R.; Scalmani, G.; Barone, V.; Mennucci, B.; Petersson, G. A.; Nakatsuji, H.; Caricato, M.; Li, X.; Hratchian, H. P.; Izmaylov, A. F.; Bloino, J.; Zheng, G.; Sonnenberg, J. L.; Hada, M.; Ehara, M.; Toyota, K.; Fukuda, R.; Hasegawa, J.; Ishida, M.; Nakajima, T.; Honda, Y.; Kitao, O.; Nakai, H.; Vreven, T.; Montgomery, J. A.; , Jr., Peralta, J. E.; Ogliaro, F.; Bearpark, M.; Heyd, J. J.; Brothers, E.; Kudin, K. N.; Staroverov, V. N.; Keith, T.; Kobayashi, R.; Normand, J.; Raghavachari, K.; Rendell, A.; Burant, J. C.; Iyengar, S. S.; Tomasi, J.; Cossi, M.; Rega, N.; Millam, J. M.; Klene, M.; Knox, J. E.; Cross, J. B.; Bakken, V.; Adamo, C.; Jaramillo, J.; Gomperts, R.; Stratmann, R. E.; Yazyev, O.; Austin, A. J.; Cammi, R.; Pomelli, C.; Ochterski, J. W.; Martin, R. L.; Morokuma, K.; Zakrzewski, V. G.; Voth, G. A.; Salvador, P.; Dannenberg, J. J.; Dapprich, S.; Daniels, A. D.; Farkas, O.; Foresman, J. B.; Ortiz, J. V.; Cioslowski, J.; Fox, D. J. *Gaussian 09, Revision B.01*; Gaussian, Inc.: Wallingford, CT, 2010.
(78) Feller, D. *J. Comput. Chem.* **1996**, *17*, 1571−1586.
(79) Schuchardt, K. L.; Didier, B. T.; Elsethagen, T.; Sun, L.; Gurumoorthi, V.; Chase, J.; Li, J.; Windus, T. *J. Chem. Inf. Model.* **2007**, *47*, 1045−1052.
(80) Seidl, A.; Görling, A.; Vogl, P.; Majewski, J. A.; Levy, M. *Phys. Rev. B* **1996**, *53*, 3764.
(81) Wheeler, S. E.; Houk, K. N. *J. Chem. Theory Comput.* **2010**, *6*, 395.
(82) Houalla, D.; Sanchez, M.; Wolf, R.; Osman, F. H. *Tetrahedron Lett.* **1978**, 4675−4678.
(83) Milbrath, D. S.; Verkade, J. G. *J. Am. Chem. Soc.* **1977**, *99*, 6607.
(84) Treichel, P. M.; Goodrich, R. A.; Pierce, S. B. *J. Am. Chem. Soc.* **1967**, *89*, 2017−2022.
(85) Goodrich, R. A.; Treichel, P. M. *Inorg. Chem.* **1968**, *7*, 694−698.
(86) Harman, J. S.; Sharp, D. W. A. *J. Chem. Soc. A* **1970**, 1935−1938.
(87) Quin, L. D.; Roser, C. E. *J. Org. Chem.* **1974**, *39*, 3423−3424.
(88) Mosbo, J. A.; Verkade, J. G. *J. Am. Chem. Soc.* **1973**, *95*, 204−209.
(89) Narayanan, K. S.; Berlin, K. D. *J. Am. Chem. Soc.* **1979**, *101*, 109−116.
(90) Vande-Griend, L. J.; Verkade, J. G.; Pennings, J. F. M.; Buck, H. M. *J. Am. Chem. Soc.* **1977**, *99*, 2459.
(91) Nifantiev, E. E.; Sorokina, S. F.; Borisenko, A. A.; Zavalishina, A. I.; Vorobjeva, L. A. *Tetrahedron* **1981**, *37*, 3183−3194.

(92) Lynden-Bell, R. M. *Trans. Faraday Soc.* **1961**, *57*, 888−892.
(93) Whitesides, G. M.; Beauchamp, J. L.; Roberts, J. D. *J. Am. Chem. Soc.* **1963**, *85*, 2665−2666.
(94) Becke, A. D. *Phys. Rev. A* **1988**, *38*, 3098−3100.
(95) Lee, C.; Yang, W.; Parr, R. G. *Phys. Rev. B* **1988**, *37*, 785−789.
(96) Miehlich, B.; Savin, A.; Stoll, H.; Preuss, H. *Chem. Phys. Lett.* **1989**, *157*, 200−206.
(97) Perdew, J. P. *Phys. Rev. B* **1986**, *33*, 8822−8824.
(98) Adamo, C.; Barone, V. *J. Chem. Phys.* **1998**, *108*, 664−675.
(99) Perdew, J. P.; Chevary, J. A.; Vosko, S. H.; Jackson, K. A.; Pederson, M. R.; Singh, D. J.; Fiolhais, C. *Phys. Rev. B* **1992**, *46*, 6671−6687.
(100) Perdew, J. P.; Wang, Y. *Phys. Rev. B* **1992**, *45*, 13244−13249.
(101) Perdew, J. P.; Burke, K.; Wang, Y. *Phys. Rev. B* **1996**, *54*, 16533−16539.
(102) Tao, J. M.; Perdew, J. P.; Staroverov, V. N.; Scuseria, G. E. *Phys. Rev. Lett.* **2003**, *91*, 146401.
(103) Sauer, S. P. A.; Raynes, W. T. *J. Chem. Phys.* **2000**, *113*, 3121.
(104) Moncho, S.; Autschbach, J. *J. Chem. Theory Comput.* **2010**, *6*, 223−234.
(105) Miertuš, S.; Scrocco, E.; Tomasi, J. *Chem. Phys.* **1981**, *55*, 117.
(106) Cancès, E.; Mennucci, B.; Tomasi, J. *J. Chem. Phys.* **1997**, *107*, 3042.
(107) Auer, A. A.; Gauss, J. *Chem. Phys.* **2009**, *356*, 7−13.
(108) Hricovini, M. *J. Phys. Chem. B* **2011**, *115*, 1503−1511.
(109) Pecul, M.; Ruud, K. *Magn. Reson. Chem.* **2004**, *42*, S128S137.